Importance of Macromixing in Batch Cooling Crystallization

Martin Bohlin and Åke C. Rasmuson
Dept. of Chemical Engineering and Technology, Royal Institute of Technology, S-100 44 Stockholm, Sweden

The importance of spatial variations of the conditions in industrial-scale, agitated, batch cooling crystallizers is investigated by computer simulations. A three-compartment model is developed considering primary and magma density-dependent secondary nucleation. An increasing crystallizer size is described by an increasing suspension turnover time. It is shown that accumulation of larger crystals in the bottom region, localized supersaturation generation and variations in the secondary nucleation rate due to varying local mixing intensity will, under normal conditions, exert a low and often negligible influence on the product-size distribution of an industrial unit. In a batch process, the product-size distribution is governed mainly by the conditions early in the process. During this period the supersaturation half-life is much longer than the suspension turnover time, and the influence of local variations becomes weak.

Introduction

Batch cooling crystallizations are commonly used in the production of fine chemicals and pharmaceuticals. The standard equipment configuration is an agitated vessel. In modeling and analysis of agitated batch cooling crystallizers, the entire volume is usually assumed to be well mixed. Whether this is a reasonable assumption or not for industrial units has not been analyzed.

The supersaturation varies within an indirectly cooled agitated crystallizer. Supersaturation is generated locally at heat-transfer surfaces, but is consumed by crystal growth in the entire volume. The rate of consumption depends on the local, total crystal surface area. The crystal growth rate and in particular the nucleation rate depend strongly on supersaturation. In a well-mixed batch cooling crystallizer, the product size distribution is sensitive to changes in supersaturation, nucleation and growth kinetics, and processing conditions (Bohlin and Rasmuson, 1992a). Garside (1985) estimated the supersaturation half-life (that is, the time needed to deplete the supersaturation to half its initial value) in continuous crystallizers. Values range from a few seconds to a few minutes at normal conditions. This is in the same range as fluid turnover times in large agitated vessels. Hence, the supersaturation decay over the fluid circulation loop can be significant in industrial continuous crystallizers. It was concluded that design procedures assuming good mixing in the liquid phase, and equal nucleation and growth rate throughout the vessel volume may be in serious error.

The size distribution and concentration of particles vary within an agitated suspension. In batch cooling crystallization, often the optimal agitation is the minimum stirring rate needed to keep all crystals just suspended from the bottom. At such conditions, a homogeneous suspension is not obtained, but especially axial variations in particle concentration and size distribution are significant (Zwietering, 1958; Nienow, 1968; Ayazi Shamlou and Zolfagharian, 1987; Baldi et al., 1978, Mersmann and Laufhütte, 1985, Ayazi Shamlou and Koutsakos, 1989; Bilek and Rieger, 1990; Bohnet and Niesmak, 1980; Baldi et al., 1981). The hydrodynamics vary significantly in an agitated liquid. The local energy dissipation rate may vary by two orders of magnitude (Mersmann et al., 1986; Laufhütte and Mersmann, 1987; Geisler and Mersmann, 1988; Jaworski and Fort, 1991; Kresta and Wood, 1993), and the highest values are found close to the agitator. Results indicate that the rate of secondary nucleation is approximately proportional to the mean specific power input to the fluid (Garside and Davey, 1980). It is thus likely that the rate of secondary nucleation may vary significantly within the tank.

There are obviously good reasons to be concerned about the assumption that an industrial batch cooling crystallizer

Correspondence concerning this article should be addressed to Å. C. Rasmuson.

can be treated as well-mixed. Unfortunately, a rigorous mathematical treatment of a nonideally mixed, agitated, instationary cooling crystallizer, becomes very complex. The fluid flow is three-dimensional and the local particle-size distribution depends on the fluid hydrodynamics. The nucleation and growth rates depend on the local supersaturation that results from local generation and consumption. Local consumption of supersaturation depends on the local size distribution. Simulation of the flow field and particle transportation, without considering crystallization, has been carried out (Brown and Boysan, 1990; Hallas and Hannan, 1990). By compartment modeling the system is decomposed into several idealized regions. Tavare (1986) summarizes the work on tank-in-series modeling of continuous crystallizers. Wiker and Anshus (1974), Dorokhov et al. (1989), and Grootscholten et al. (1982) used compartment modeling to study macromixing effects in evaporation loop crystallizers. Significant influence of crystallizer geometry and internal circulation rate on the crystal-size distribution (CSD) was found. Kratz and Hoyer (1989) suggest a scale-up method based on a loop model. Jager et al. (1991) modeled the effect of scale of operation on CSD dynamics, and the results were used to explain oscillatory behavior of a continuous evaporation unit.

The objective of this article is to investigate whether it is reasonable to model an industrial batch cooling crystallizer as a well-mixed process. The influence on the product crystal-size distribution of spatial variations in specific turbulence energy dissipation rate, supersaturation generation, and size distribution and concentration of crystals are analyzed.

Model

Consider a jacketed, draft-tubed, baffled tank crystallizer equipped with an axial-flow impeller (Figure 1). Divide the tank volume into three well-mixed compartments. The first compartment denoted C1 is the region where cooling occurs and supersaturation is generated. The second compartment C2 is located around the impeller where the turbulence energy dissipation rate is particularly high. In the third compartment C3 which forms the lower part of the tank, the magma density may be particularly high, due to gravity.

Assume that the three compartments C1, C2, and C3 form a closed loop-reactor where the flow of particles and liquid is in only one direction as shown in Figure 1. The concept of macrofluid (Levenspiel, 1972) is applied, that is, the fluid is assumed to consist of small elements, which retain their identity during the process. The elements have a physical volume, small compared to the total tank volume, but large enough to have average values of intensive properties such as concentration, temperature, population density distribution, and specific energy dissipation rate. It is assumed that the elements travel around the loop completely segregated from each other, that is, there is no exchange of particles, solvent, solute or energy between the elements. The flow around the loop is orderly with no element overtaking any other element, ahead or behind. All elements have equal turnover times τ_{tot}, that is, the time to travel through the loop, and have equal residence times τ_1, τ_2 and τ_3 in each respective compartment. The temperature of compartment C1 is strictly controlled, and is given by a predetermined temperature vs. time profile:

$$(\theta_o - \theta)/(\theta_o - \theta_f) = (t/t_f)^a \tag{1}$$

The element receives the temperature θ when entering compartment C1 in which the temperature is assumed to be uniform. In compartments C2 and C3 it is assumed that the temperature of the element remains constant, equal to the temperature received at the moment of exit from C1. At the reentrance to C1, the temperature immediately drops to the prevailing θ-value.

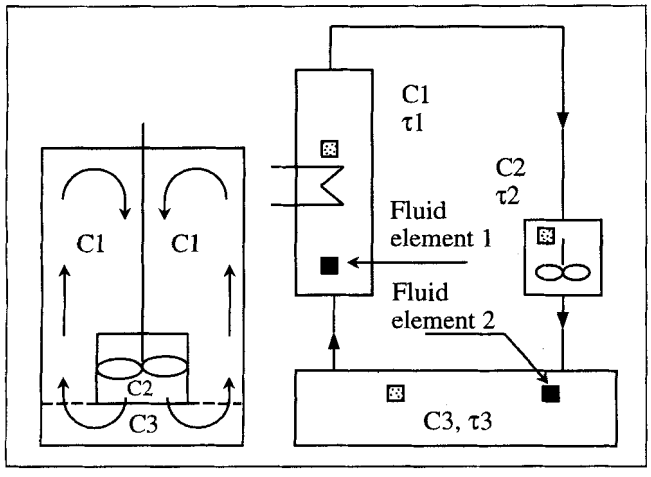

Figure 1. Compartment model of the agitated vessel.

Modeling of circulating homogeneous suspension

Consider the case where all crystals are evenly distributed in the fluid (homogeneous suspension) however with spatial variations in supersaturation and mixing energy dissipation rate. The individual suspension elements can be assumed to act as small, well-mixed batch reactors having constant solvent mass, a time varying secondary nucleation rate constant, and a discontinuous temperature curve. It is assumed that crystal breakage, agglomeration and growth rate dispersion can be neglected, and that crystals are born at zero size. The population balance for an element then becomes (Randolph and Larson, 1988)

$$\frac{\partial n}{\partial t} + \frac{\partial (n \cdot G)}{\partial L} = 0 \tag{2}$$

This equation can be solved by a solution algorithm that discretizes the crystal generation process into subpopulations of particles. Using the method of characteristics, these subpopulations are traced as they move along the size axis at the rate of crystal growth $G(t, L)$ (Bohlin and Rasmuson, 1992a,b). The number of crystals in the ith subpopulation N_i, is the integral of the total nucleation rate over the time interval Δt:

$$N_i = \int_{t_i}^{t_i + \Delta t} [B_p + B_s] dt \tag{3}$$

where t_i is the birth time of subpopulation i and $t_1 = 0$. In each time interval a new subpopulation is generated. Seeds

are added at $t = 0$, and receive $i = 0$. The primary and secondary nucleation rates are described by power laws:

$$B_p = k_p \cdot \Delta c^{n_p} \tag{4}$$

$$B_s = k_s(t) \cdot W_T^b \cdot \Delta c^{n_s} \tag{5}$$

where the secondary nucleation rate constant k_s is a function of time, since the element is subjected to different specific energy dissipation rates in the different compartments. The linear growth rate G may be size-dependent:

$$G = \frac{dL_i}{dt} = k_g \cdot (\gamma + \alpha \cdot L_i)^{\beta} \cdot \Delta c^{g} \tag{6}$$

and the size of the crystals in the ith subpopulation at time t becomes

$$L_i(t) = L_i(t = 0) + \int_{t_i}^{t} G(t)dt \tag{7}$$

For nucleated crystals, $L_i\ (t = 0) = 0\ (i > 0)$. For seeded crystals $L_o\ (t = 0) = L_{so}$. The global process time t is the total time since the start of the batch, whereas the loop time τ is equal to the time elapsed after the entrance to C1 of each turn. The population balance is coupled to the supersaturation balance for the element by the third moment of the total size distribution:

$$\frac{d\Delta c}{dt} = -\frac{dc_{eq}}{dt} - \frac{dW_T}{dt}; \quad \Delta c(t = 0) = \Delta c_o \tag{8}$$

where

$$W_T(t) = k_v \cdot \rho_c \cdot m_3(t) = k_v \cdot \rho_c \cdot \sum_{i=0}^{k} N_i \cdot L_i^3(t) \tag{9}$$

To simulate the influence of spatial variations in supersaturation generation and mixing energy dissipation rate in a homogeneous suspension, one circulating element is analyzed. The product of the entire batch is assumed to be well characterized by the properties of this element.

Modeling of a circulating nonhomogeneous suspension

Uneven distribution of crystals (nonhomogeneous suspension) is modeled as follows: Those crystals in a circulating element that are or become larger than a certain size $L_{\max}$ during the stay of the element in compartment C3 (that is, when $\tau > \tau_1 + \tau_2$), are removed from the element and retained in C3, at the moment when the element leaves this compartment. When the element returns into C3, the crystals retained in this compartment are added for the time period the element rests in C3 (τ_3). The crystals retained in C3 must grow continuously (that is, also when the element rests in C1 or C2), like those crystals that travel with the element around the loop. This is achieved in the model by considering additional elements that take over from one another in compartment C3. The number of elements needed to achieve continuous growth of crystals retained in C3, depends on the residence time distribution. We may define a parameter X as

$$X = (V_1 + V_2 + V_3)/V_3 = (\tau_1 + \tau_2 + \tau_3)/\tau_3 \tag{11}$$

which specifies the number of circulating elements needed. For example, when $V_1 + V_2 = V_3$, X equals 2, and two circulating elements are included in the analysis. They replace one another in C3 and only one element at a time stays in C3. The elements are to be positioned evenly around the loop as illustrated in Figure 1 for $X = 2$. Both elements deposit large crystals in C3. Each element contacts all crystals retained in C3 (that is, all crystals deposited by all elements) for the entire residence time in that compartment. By this, the model accounts for an increased magma density in C3.

The number of crystals in the ith subpopulation in the jth circulating element becomes

$$N_{j,i}(t) = (1-h) \cdot \int_{t_{j,i}}^{t_{j,i}+\Delta t} [B_p + B_s]dt \quad \begin{cases} h = 0; & L_{j,i} \le L_{\max} \\ h = 1; & L_{j,i} > L_{\max} \end{cases} \tag{3'}$$

h is used to remove large crystals from the element and is only activated (that is, allowed to receive the value of unity) at the moment the element leaves C3. The size of the crystals is

$$L_{j,i}(t) = L_{j,i}(t = 0) + \int_{t_{j,i}}^{t} G(t)dt \tag{7'}$$

The number of incompletely suspended crystals in C3 originating from the ith subpopulation in the jth element is

$$N_{j,i}^*(t) = h \cdot \int_{t_{j,i}}^{t_{j,i}+\Delta t} [B_p + B_s]dt \quad \begin{cases} h = 0; & L_{j,i} \le L_{\max} \\ h = 1; & L_{j,i} > L_{\max} \end{cases} \tag{12}$$

with the same conditions for h as above. The size of the crystals in the subpopulation $L_{j,i}^* = L_{j,i}$ is still calculated by Eq. 7′ but with different $G(t)$. The supersaturation balance for the jth element is

$$\frac{d\Delta c_j}{dt} = -\frac{dc_{eq,j}}{dt} - \frac{d(W_{T,j} + W_T^*)}{dt} \tag{8'}$$

where $W_{T,j}$ is the magma density in the jth element:

$$W_{T,j}(t) = k_v \cdot \rho_c \cdot m_{j,3}(t) = k_v \cdot \rho_c \cdot \sum_{i=0}^{k} N_{j,i} \cdot L_{j,i}^3(t) \tag{9'}$$

and W_T^* is the magma density resulting from the retained crystals in C3. By definition, $W_T^* = 0$ in compartments C1 and C2. The magma density of the crystals which are retained in compartment C3, when these are added to the element, becomes

$$W_T^* = \begin{cases} 0; & \tau \le \tau_1 + \tau_2 \\ k_v \rho_c \sum_{j=1}^{X} \sum_{i=0}^{k} N_{j,i}^* \cdot (L_{j,i}^*)^3; & \tau > \tau_1 + \tau_2 \end{cases} \quad (9'')$$

The history of different elements (temperature, supersaturation, nucleation and growth rates, and so on) is almost identical, and accordingly the final product size distribution of the elements becomes very close. The overall product-size distribution is obtained by averaging over the distributions of the individual elements. At nonhomogeneous suspending, the crystals partitioned off in the bottom compartment are accounted for, as is described below.

Numerical solution

In the case of a homogeneous suspension, the element is initially positioned in C1. In the case of a nonhomogeneous suspension, X elements are initially placed evenly around the loop, thus receiving different initial local loop times, but the initial temperature and supersaturation are equal (see Figure 1 for $X = 2$). In case of seeding, all elements initially receive equal amount of seeds. Solution of the model involves integration of Eqs. 3 and 8 (or 3′ and 8′) by Euler's method. In each time step, Eq. 3 (3′) is solved for the number of crystals in the subpopulation. Then the change of the crystal size and mass is calculated by using Eqs. 7 and 9 (7′, 9′ and 9″). Finally, the supersaturation balance Eq. 8 (8′) is solved for the supersaturation.

At short turnover times, short time steps are required due to the short residence time in the compartment C2. Especially, in case of short turnover times in combination with a long total process time, there is a need for a large computer memory and high processing speed. Hence, there is a lower limit to the turnover times that has been studied. Most simulations have been performed on a Macintosh IIfx, and a few on a workstation Hewlett Packard 9000/720. Time steps of 1 s (0.5 s in a few cases) are normally used for the calculations in this study. Further refinement of the time discretization does not significantly change the results presented.

Complete population density distributions can be estimated from the discrete size distributions. In this article, however, the total size distributions are characterized by the weight mean size and the corresponding coefficient of variation (CV). These are calculated directly from the total moments of the product-size distribution (Randolph and Larson, 1988). For the case of homogeneous suspension:

$$L_{wm} = \frac{m_4}{m_3} \quad (13)$$

$$\sigma_{wm}^2 = \frac{m_5}{m_3} - \left[\frac{m_4}{m_3}\right]^2 \quad (14)$$

in which the n'th moment is calculated as

$$m_n = \sum_{i=0}^{k} N_i L_i^n \quad (15)$$

For the case of nonhomogeneous suspension, we account also for the size distribution of the incompletely suspended crystals. The moments of the total distribution can be obtained by summation of the corresponding moments of individual distributions (Bohlin and Rasmuson, 1992b). The mean size is obtained by

$$L_{wm} = \frac{\frac{1}{X}\sum_{j=1}^{X} [m_{j,4}^* + m_{j,4}]}{\frac{1}{X}\sum_{j=1}^{X} [m_{j,3}^* + m_{j,3}]} \quad (13')$$

and the variance of the distribution is calculated according to

$$\sigma_{wm}^2 = \frac{\frac{1}{X}\sum_{j=1}^{X} [m_{j,5}^* + m_{j,5}]}{\frac{1}{X}\sum_{j=1}^{X} [m_{j,3}^* + m_{j,3}]} - \left[\frac{\frac{1}{X}\sum_{j=1}^{X} [m_{j,4}^* + m_{j,4}]}{\frac{1}{X}\sum_{j=1}^{X} [m_{j,3}^* + m_{j,3}]}\right]^2 \quad (14')$$

The nth moment of the size distribution in the jth circulating element is

$$m_{j,n} = \sum_{i=0}^{k} N_{j,i} L_{j,i}^n \quad (15')$$

The moment of the incompletely suspended crystals originating from the jth element is

$$m_{j,n}^* = \sum_{i=0}^{k} N_{j,i}^* (L_{j,i}^*)^n \quad (15'')$$

For homogeneous as well as nonhomogeneous suspension the coefficient of variation is calculated by

$$CV_{wm} = \sigma_{wm}/L_{wm}. \quad (16)$$

Simulations

The influence of macroscopic spatial variations in the generation of supersaturation in the rate constant of secondary nucleation and in the crystal-size distribution are investigated. The specific set of parameters used in the simulations are given in Table 1. Kinetic parameters are based on (Bohlin and Rasmuson, 1992a) data for potassium sulfate. The operating conditions are such that the process behaves like a normal batch cooling crystallization, that is, typical peaks appear in supersaturation and nucleation rate vs. time (see Figure 1 of Bohlin and Rasmuson, 1992b). A linear cooling profile ($a = 1$) is used in the simulations if not otherwise stated. Whenever used, seeds are added at $t = 0$ in an amount corresponding to approximately 1.4% of the final crystallized mass. The secondary nucleation rate constant is assumed to be proportional to the specific turbulence energy dissipation rate of each compartment. Mersmann et al. (1986) determined local

Table 1. Parameter Values Used in the Simulations

Parameter	Value	Parameter	Value
Batch time, t_f	8,000	Primary nucl. rate const., k_p	6.68×10^{17}*
Start temp., θ_o	60	Primary nucl. rate order, n_p	7.63*
Final temp., θ_f	25	Secondary nucl. rate const. C1, k_{s1}	5.29×10^{5}†
Solubility const., c_o	0.0666**	Secondary nucl. rate const. C2, k_{s2}	5.29×10^{6}
Solubility const., c_1	0.0023**	Secondary nucl. rate const. C3, k_{s3}	8.82×10^{5}
Solubility const., c_2	-6.0×10^{-6}**	Secondary nucl. rate order, n_s	0.69†
Crystal density, ρ_c	2,662**	Exponent of magma dens. dep., b	0.5†
Shape factor, k_v	0.525***	Growth rate constant, k_g	6.0×10^{-7}†
No. of seeds, N_s	5,000	Factor of size dependence, α	0.443†
Size of seeds, L_{so}	0.5×10^{-3}	Exponent of size dependence, β	0.778†
		Growth rate order, g	1.288†
		Constant, γ	300

*Jones and Mullin (1974); **Mullin (1972); ***Tavare and Chivate (1977); †Randolph and Sikdar (1976), ‡second-order polynomial fit to published data: $c_{eq} = c_o + c_1\cdot\theta + c_2\cdot\theta^2$.

energy dissipation rates in an agitated tank. Based on those results, the local secondary nucleation rate constants in the compartments are chosen as: $k_{s1} : k_{s2} : k_{s3} = 0.6 : 6 : 1$, and are kept constant in the simulations, except for when the influence of kinetics is examined. The energy dissipation rate measurements also indicate reasonable relative sizes: V_1, V_2 and V_3 of the compartments. Residence times in compartments are calculated by

$$\tau_1 = \frac{V_1}{V_{tot}}\cdot\tau_{tot};\quad \tau_2 = \frac{V_2}{V_{tot}}\cdot\tau_{tot};\quad \tau_3 = \frac{V_3}{V_{tot}}\cdot\tau_{tot} \quad (17a\text{–}c)$$

The residence time distribution of nonhomogeneous suspension processes are chosen such that $X = 2$ in Eq. 11. Thus, it is sufficient to include two circulating fluid elements. Results are presented in which the total turnover time is increased while keeping crystallization kinetics and the ratios τ_i/τ_{tot} constant. An increasing total turnover time is aimed to represent an increasing crystallizer size. Results are compared with well-mixed crystallizers, the results of which are presented in diagrams at zero turnover time. The residence time averaged, secondary nucleation rate constant of the nonwellmixed process

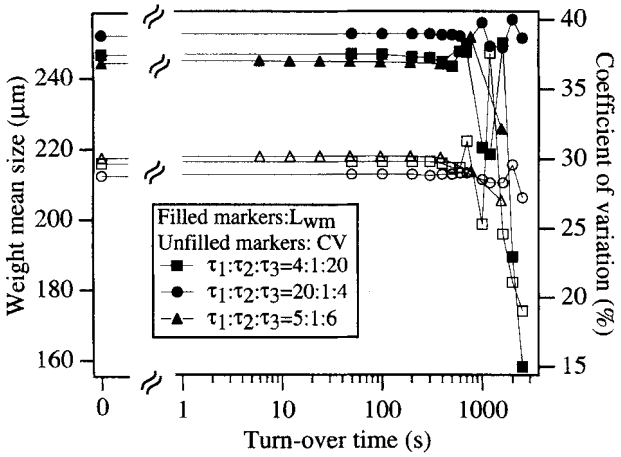

Figure 2. Influence of turnover time and residence time distribution on product characteristics.

Homogeneous suspension, unseeded process: -■- $k_s = 1.136\ k_{s3}$; -●- $\bar{k}_s = 0.88\ k_{s3}$; -▲- $\bar{k}_s = 1.25\ k_{s3}$.

$$\bar{k}_s = [\Sigma k_{si}\cdot\tau_i]/\tau_{tot} \quad (18)$$

is used in simulation of the well-mixed crystallizer to obtain equal crystallization kinetics. The simulations include a range of combinations of residence times and, consequently, this average value varies somewhat between different series of simulations. In the diagrams for nonhomogeneous suspending, results for zero turnover time is for a crystallizer that is entirely well-mixed, that is, the suspension is homogeneous also. The minimum turnover time considered is 6 s in the case of homogeneous suspension, and 12.5 s in the case of nonhomogeneous suspension. In total, this article is based on about 125 simulations for potassium sulfate. In addition, about 120 simulations have been made for batch cooling crystallization of citric acid monohydrate (for kinetics see Bohlin and Rasmuson, 1992a).

Results

Results are shown in Figure 2 for an unseeded process where the suspension is homogeneous, but spatial variations in supersaturation generation and mixing energy dissipation rate, are at hand. Product weight mean size and the corresponding coefficient of variation is plotted vs. turnover time. Three cases are presented having different residence time distributions. The logarithmic time scale is interrupted to allow results of zero turnover time, that is, ideal mixing, to be displayed. The results show that the influence of turnover time on the product properties is negligible below 500 s, regardless of residence time distribution. There is a slight influence of the residence time distribution, which is due to an influence on the time averaged, secondary nucleation rate constant according to Eq. 18. Turnover times in the range of 500 s are an order of magnitude higher than average turnover times in large industrial agitated crystallizers, and are approaching the order of magnitude of the total process time in the simulations: 8,000 s.

Results for a nonhomogeneous suspension are presented in Figure 3 for different levels of suspending. The crystal size at which settling out from the circulating element occurs: L_{max} is 80, 200 or 300 μm, or infinity which corresponds to the case of homogeneous suspension. Again the results show that the influence of turnover time on the product properties is weak. However, nonhomogeneous suspending does increase the sensitivity to variations along the circulation path. The process becomes increasingly more sensitive to turnover time

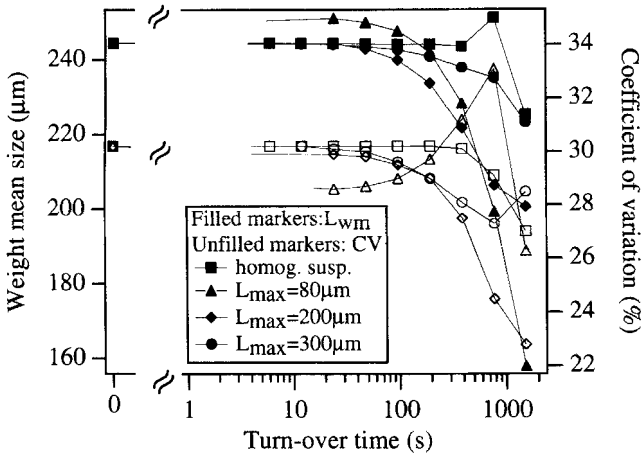

Figure 3. Influence of turnover time and suspending on product characteristics.

Residence time distribution: $\tau 1{:}\tau 2{:}\tau 3 = 5{:}1{:}6$; unseeded process: $\bar{k}_s = 1.25\ k_{s3}$.

at decreasing value of L_{max}, even though the influence of L_{max} is not entirely regular. At $L_{max} = 80\ \mu$m the product deviates from the well-mixed reference case already at the shortest turnover time investigated. However, the deviation is less than 5% until τ_{tot} exceeds a few hundred seconds. At $L_{max} \geq 200\ \mu$m, deviations can be observed at $\tau_{tot} > 40$–50 s and become important at $\tau_{tot} > 200$ s. At decreasing L_{max}, the relative mass of nonhomogeneously suspended crystals increases. For the 300 μm limit about 1.5% of the final product mass is found in C3, which explains the relatively small deviation from the well-mixed case. At $L_{max} = 200\ \mu$m approximately two-thirds of the crystal mass is nonhomogeneously suspended at the end of the process. In view of the product mean sizes of the processes presented in Figure 3, $L_{max} = 80\ \mu$m is regarded as a very low limit of homogeneous suspending, corresponding to inadequate design of the agitation.

The insensitivity of the product-size distribution to suspension turnover time is not limited to the processing conditions and the crystallization kinetics of the simulations presented. Seeding increases the importance of nonhomogeneous suspending. Deviations from the well-mixed case appear already at the shortest turnover time ($\tau_{tot} = 12$ s), but the differences observed exceed 5–15%, only at turnover times above a few hundred seconds. The influence of an increasing turnover time is weak also when a controlled colling curve is applied ($a = 3$ in Eq. 1). If the total process time becomes shorter, the changes in product properties do show up at a shorter turnover time; however, still at approximately the same ratio of turnover time to overall batch time. There is no principal difference between the results for potassium sulfate (low magma density system) and those for citric acid monohydrate (high magma density system), concerning the sensitivity to spatial variations in the crystallizer. Simulations at homogeneous suspending reveal that an unseeded process with negligible secondary nucleation, that is, $k_s = 0$, as well as a seeded process with negligible primary nucleation, that is, $k_p = 0$, or having 10 times higher growth rate, still are very weakly influenced by the turnover time. No increase in sensitivity to the turnover time has been found at an increased variation of the energy dissipation rate.

Discussion

The results presented clearly suggest that at turnover times up to a few hundred seconds, spatial variations in supersaturation generation, in the secondary nucleation rate constant and in particle-size distribution, have a low and usually negligible effect on the product-size distribution of batch cooling crystallization. Turnover time usually increases with size of agitated tanks, from 0.2 s in a 6.3 L crystallizer, to 60–70 s in a 50 m^3 unit (Garside, 1985; Heffels, 1986; Jager et al., 1991). Hence, the results suggest that the influence of spatial variations is low, not only in small laboratory crystallizers, but also in large industrial units.

Figure 4 shows the supersaturation curves for some of the seeded processes, exhibiting nonhomogeneous suspending. The seed crystals are retained from the start in C3. The smooth, unbroken line represents the well-mixed process and the supersaturation curve has the bell shape that is typical for batch cooling crystallization processes. At short turnover times, the only influence of spatial variations is a slight overshoot in the maximum value. At longer turnover times a serrated curve is obtained but a major influence on the overall bell shape is only seen at exceedingly long turnover times. The local supersaturation is determined by the rate of generation of supersaturation in compartment C1, and by the rate of consumption, being directly proportional to the available total, local, crystal surface area. The rate of consumption can be described by the supersaturation half-life:

$$t_{half}(t_i) = \frac{\Delta c_i/2}{\Delta W_{T,i}/\Delta t} \tag{21}$$

in which Δc_i is the supersaturation in the beginning of each time step, and $\Delta W_{T,i}/\Delta t$ is the calculated rate of mass consumption during the time step. Figure 5 shows the calculated half-life vs. process time (t) for the process having 384 s turnover time and for the ideal mixing case. During the first part of the batch, the total crystal surface area in the element is low. Hence, the rate of supersaturation consumption in the

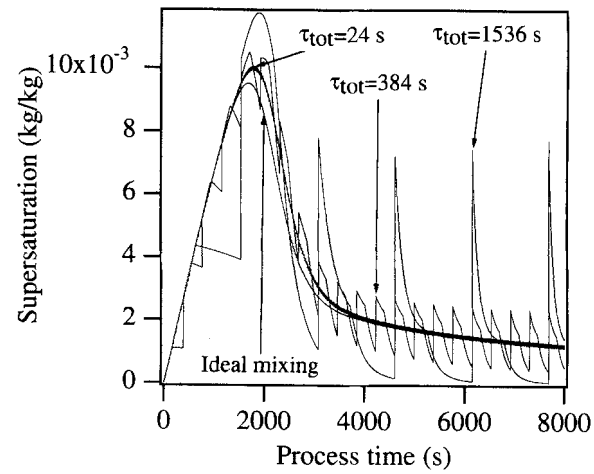

Figure 4. Influence of turnover time on supersaturation vs. process time.

Residence time distribution: $\tau 1{:}\tau 2{:}\tau 3 = 5{:}1{:}6$; well-mixed process and nonhomogeneous suspension ($L_{max} = 500\ \mu$m); seeded processes: $\bar{k}_s = 1.25\ k_{s3}$.

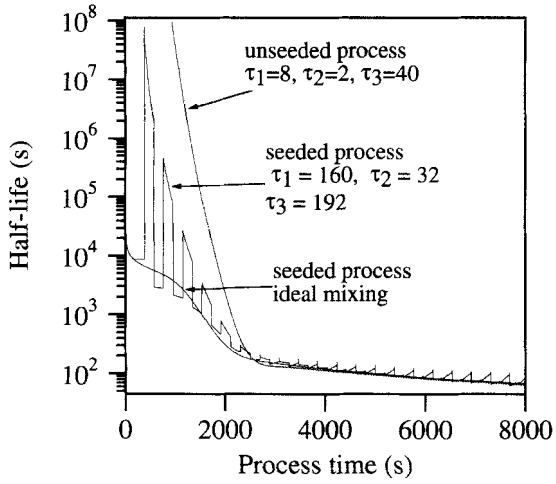

Figure 5. Supersaturation half-life time vs. process time.

Homogeneous suspension/unseeded process, $\bar{k}_s = 1.136\ k_{s3}$; ideal mixing and nonhomogeneous suspension/seeded processes, $\bar{k}_s = 1.25\ k_{s3}$.

element is low and the half-life is long. A significant supersaturation decay may take place in compartment C2 and C3, only at very long turnover times. t_{half} increases when the element leaves C3 and decreases again at the reentrance to C3, since the crystal surface area is higher in C3 than in C2 and C1. However, in comparison to the well-mixed case, the surface area in C3 is only higher because crystals are accumulated in a reduced volume. Hence, t_{half} in C3 will under normal conditions only be moderately reduced. During the process, the half-life decreases with increasing total crystal surface area, and the fluctuations decrease as an increasing crystal surface area travels with the element around the loop. Also shown in Figure 5 is an unseeded process at homogeneous suspending. The half-life curves for $\tau_{tot} = 0$ (i.e., ideal mixing), $\tau_{tot} = 50$, and $\tau_{tot} = 100$ s are very close, and fluctuations because of spatial variations are negligible.The importance of the variations in the nucleation rate constant is limited, since the residence time in the impeller region compartment is very short.

The product-size distribution of batch cooling crystallization depends strongly on the conditions early in the process. The crystals born during the period of early nucleation or added as seeds tend to dominate the product mass. Product properties are insensitive to spatial variations of the conditions, because the magma density early is low. The overall bell shape of the supersaturation profile is only weakly influenced, and the supersaturation half-life is significantly longer than the fluid turnover time during most of the process. Nonhomogeneous suspending may become important if a major crystal surface area is incompletely suspended early in the process, that is, if even very small crystals are nonhomogeneously suspended, or when a significant mass of nonhomogeneously suspended seeds is added.

The results of this study suggest that spatial variations, as a first and often very good approximation can be neglected in modeling of industrial batch cooling crystallizers, that is, the industrial process can be assumed to be well-mixed. In addition, spatial variations are unlikely to contribute significantly to broadening of size distributions. Turnover time distributions can be fairly wide in agitated liquids (Hallas and Hannan, 1990). However, since the influence of average turnover time on the product is very weak; also a distribution of turnover times should have a low influence. Garside (1985) concluded that in an industrial continuous crystallizer, spatial variations may have a significant influence on the product. However, the continuous process is operated at a constant, often high magma density, and t_{half} may be close to or even lower than the turnover time. In a continuous evaporative crystallizer, the solution may actually become undersaturated in the heat exchanger. Small crystals may dissolve completely, resulting in an oscillating product mean size especially in large units (Jager et al., 1991). This suggests that our conclusions concerning the influence of macromixing in a batch cooling crystallizer should not be extrapolated uncritically to batch evaporation crystallizers.

The product characteristics of a batch cooling crystallizer are sensitive to the crystallization kinetics. Secondary nucleation is approximately proportional to the mean specific power input to the fluid (Garside and Davey, 1980), and the growth rate increases with mean specific power input raised to no more than 0.2 (Levins and Glastonbury, 1972). In the present work, the crystallization kinetics are kept constant, when the turnover time increases. This is reasonable, only if the specific power input remains constant. In practice, especially in crystallization processes, turnover time normally increases with vessel size, while specific power input decreases. Hence, especially the rate of secondary nucleation tends to be lower in larger vessels having a longer turnover time. However, this is a direct effect on kinetics that would influence the product, regardless of if the crystallizer is well-mixed or not. The present study focuses on whether large batch cooling crystallizers in which spatial variations can develop because of long turnover times and nonhomogeneous suspending can be assumed to be well-mixed. The focus is not primarily on scale-up. In the modeling, complete segregation is assumed. However, an exchange of particles, heat, and solute between different elements is likely to decrease the effects of circulation and maldistribution. The model does not consider the influence of varying mixing energy dissipation on the rate of crystal growth, because the dependence is considerably much weaker than that of secondary nucleation. The effects of extreme spatial variations, such as completely stagnant regions, solids deposition onto the bottom, incrustation, have not been considered in this work.

Conclusions

In an industrial agitated tank applied for batch cooling crystallization, supersaturation is generated locally at heat-transfer surfaces; secondary nucleation is likely to be particularly strong in the impeller region and large crystals tend to accumulate in lower regions of the tank. The results of this study indicate that such spatial variations of the conditions in the tank will under normal conditions exert a low and often negligible influence on the product-size distribution. This distribution of a batch cooling crystallizer is mainly governed by the conditions early in the process, when the principal number of crystals that share the final mass is established. During the first part of the process, the magma density is low and the rate of local supersaturation consumption is low com-

pared to the rate of supersaturation generation. The overall supersaturation profile is only weakly influenced by spatial variations, and during most of the process the supersaturation half-life is significantly longer than the fluid turnover time. The results of this work suggest that industrial batch cooling crystallizers can, as a first and often very good approximation, be assumed to be well-mixed, if reasonably adequate agitation is provided. The results of this work also suggest that it is unlikely that spatial variations in a batch cooling crystallizer will result in significant broadening of the product-size distribution.

Acknowledgment

The financial support of The Swedish National Board for Industrial Technical Development (NUTEK), The Swedish Council for Planning and Coordination of Research (FRN) and The Swedish Industrial Association for Crystallization Research and Development (IKF) are all gratefully acknowledged.

Notation

b = empirical mass exponent
B_p = primary nucleation rate, no./s/kg solvent
B_s = secondary nucleation rate, no./s/kg solvent
c_{eq} = equilibrium concentration, kg/kg solvent
$c_{eq,j}$ = equilibrium concentration in jth element, kg/kg solvent
c_o = constant, kg/kg solvent
c_1 = constant, kg/kg solvent/°C
c_2 = constant, kg/kg solvent/(°C)^2
c_3 = constant, kg/kg solvent/(°C)^3
Δc = supersaturation, kg/kg solvent
Δc_j = supersaturation in jth element, kg/kg solvent
Δc_o = initial supersaturation, kg/kg solvent
CV = coefficient of variation, $CV = \sigma/\bar{x}$
g = growth rate order
G = linear growth rate, m/s
h = separation factor
k = number of subpopulations
k_g = growth rate constant, m/s (kg/kg)$^{-g}$
k_p = primary nucleation rate constant, no./kg (kg/kg)$^{-n_p}$
k_s = secondary nucleation rate constant, no./kg (kg/kg)$^{-n_s-b}$
k_{si} = secondary nucleation rate constant in ith compartment, no./kg (kg/kg)$^{-n}s^{-b}$
$\bar{k}_s$ = average secondary nucleation constant according to Eq. 18
k_v = volume shape factor
L = characteristic crystal dimension, m
L_i = size of ith crystal subpopulation
$L_{j,i}$ = size of ith subpopulation in jth element
$L^*_{j,i}$ = size of ith subpopulation originating from jth element
$L_{\max}$ = maximum size of complete suspension
L_{wm} = weight mean size, m
L_{so} = initial size of seeds
m_i = ith moment of size distribution
$m_{j,i}$ = ith moment of size distribution in jth element
$m^*_{j,i}$ = ith moment of separated crystals originating from the jth element
n = population density, no./kg/m
n_p = primary nucleation rate exponent
n_s = secondary nucleation rate exponent
N_i = number of crystals in ith subpopulation, no./kg
$N_{j,i}$ = number of crystals in ith subpopulation in jth element, no./kg
$N^*_{j,i}$ = number of crystals in ith subpopulation originating from jth element, no./kg
N_s = number of seed crystals, no./kg
Δt = time interval, s
t = time, s
t_f = total batch time, s
t_i = birth time of subpopulation, s
$t_{j,i}$ = birth time of ith subpopulation in jth element, s
V_i = size of ith compartment
W_T = magma density, kg/kg
$W_{T,j}$ = suspended solids concentration in jth element, kg/kg solvent
W^*_T = suspended solids concentration of crystals in C3, kg/kg solvent
X = ratio of total volume to volume of compartment C3

Greek letters

α = factor in growth rate expression
β = factor in growth rate expression
γ = factor in growth rate expression
θ_o = initial temperature, °C
θ_f = final temperature, °C
ρ_c = density of crystals, kg/m^3
σ_{wm} = standard deviation of mass distribution
τ = local time in loop, s
τ_{tot} = turnover time, s

Superscripts

$-$ = mean value of variable
$*$ = parameter related to incompletely suspended crystals

Subscripts

i = variable related to subpopulation born at time t_i
L = size distribution
s = seed

Literature Cited

Ayazi Shamlou, P., and E. Koutsakos, "Solid Suspension and Distribution in Liquids under Turbulent Agitation," *Chem. Eng. Sci.*, **44**, 529 (1989).

Ayazi Shamlou, P., and A. Zolfagharian, "Incipient Solid Motion in Liquids in Mechanically Agitated Vessels," *I. Chem.E. Symp. on Fluid Mixing III*, Bradford Univ., U.K., p. 195 (1987).

Baldi, G., R. Conti, and E. Alaria, "Complete Suspension of Particles in Mechanically Agitated Vessels," *Chem. Eng. Sci.*, **33**, 21 (1978).

Baldi, G., R. Conti, and A. Gianetto, "Concentration Profiles for Solids Suspended in a Continuous Agitated Reactor," *AIChE J.*, **27**, 1017 (1981).

Bilek, P., and F. Rieger, "Distribution of Solid Particles in a Mixed Vessel," *Coll. Czech. Chem. Comm.*, **55**, 2169 (1990).

Bohlin, M., and Å. C. Rasmuson, "Application of Controlled Cooling and Seeding in Batch Cooling Crystallisation," *Can. J. Chem. Eng.*, **70**, 120 (1992a).

Bohlin, M., and Å. C. Rasmuson, "Modeling of Growth Rate Dispersion in Batch Cooling Crystallization," *AIChE J.*, **38**, 1853 (1992b).

Bohnet, M., and G. Niesmak, "Distribution of Solids in Stirred Suspensions," *Ger. Chem. Eng.*, **3**, 57 (1980).

Brown, D. J., and F. Boysan, "The Modelling of Fluid Flow in a Stirred Sugar Crystallizer," *Industrial Crystallization*, A. Mersmann, ed., Garmisch-Partenkirchen, Germany, p. 29 (1990).

Dorokhov, I. N., and E. M. Koltsova, "Simulating Crystallization in Evaporators," *Theoretical Foundations of Chemical Engineers*, **23**, 123 (1989).

Garside, J., "Industrial Crystallization from Solution," *Chem. Eng. Sci.*, **40**, 3 (1985).

Garside, J., and R. J. Davey, "Secondary Contact Nucleation: Kinetics, Growth and Scale-Up," *Chem. Eng. Commun.*, **4**, 393 (1980).

Geisler, R. K., and A. Mersmann, "Local Velocity Distribution and Power Dissipation Rate of Suspensions in Stirred Vessels," *European Conf. on Mixing*, Pavia, Italy, p. 272 (1988).

Grootscholten, P. A. M., C. J. Asselbergs, A. Scrutton, and E. J. de Jong, "Effect of Crystallizer Geometry on Crystallizer Performance," *Industrial Crystallization*, S. J. Jancic and E. J. de Jong, eds., North-Holland Publishing Co., Amsterdam (1982).

Hallas, N. J., and M. L. Hannan, "Measurement and Computation of Hydrodynamics for a Draft Tube Baffled Crystallizer," *Industrial Crystallization*, A. Mersmann, ed., p. 107 (1990).

Heffels, S. K., "Product Size Distribution in Continuous and Batch Sucrose Crystallizers," PhD Thesis, Delft Univ. of Technology, The Netherlands (1986).

Jager, J., H. J. M. Kramer, B. Scarlett, E. J. de Jong, and S. de Wolf, "Effect of Scale of Operation on CSD Dynamics in Evaporative Crystallizers," *AIChE J.*, **37**, 182 (1991).

Jaworski, Z., and I. Fort, "Energy Dissipation Rate in a Baffled Vessel with Pitched Blade Turbine Impeller," *Coll. Czech. Chem. Commun.*, **56**, 1867 (1991).

Jones, A. G., and J. W. Mullin, "Programmed Cooling Crystallization of Potassium Sulphate Solutions," *Chem. Eng. Sci.*, **29**, 105 (1974).

Kratz, E., and F. Hoyer, "Scale up from Pilot Plant Test Data—A Simplified Numerical Approach," *Industrial Crystallization 87*, J. Nyvlt and S. Zacek, eds., Elsevier, Oxford (1989).

Kresta, S. M., and P. E. Wood, "The Flow Field Produced by a Pitched Blade Turbine: Characterization of the Turbulence and Estimation of the Dissipation Rate," *Chem. Eng. Sci.*, **48**, 1761 (1993).

Levenspiel, O., *Chemical Reaction Engineering*, 2nd ed., Wiley, New York (1972).

Levins, D. M., and J. R. Glastonbury, "Particle-Liquid Hydrodynamics and Mass Transfer in a Stirred Vessel," *Trans. Instn. Chem. Engrs.*, **50**, 132 (1972).

Laufhütte, H. D., and A. Mersmann, "Local Energy Dissipation in Agitated Turbulent Fluids and its Significance for the Design of Stirring Equipment," *Chem. Eng. Technol.*, **10**, 56 (1987).

Mersmann, A., and H. D. Laufhütte, "Scale-up of Agitated Vessels for Different Mixing Processes," *European Conf. on Mixing*, Wurzburg, West Germany, p. 273 (1985).

Mersmann, A., H. D. Laufhütte, and H. Voit, "Relation Between Fluid Dynamics and Mixing Tasks in Stirred Vessels," *World Cong. III of Chemical Engineering*, Tokyo, p. 394 (1986).

Mullin, J. W., *Crystallization*, 2nd ed., Butterworth, London (1972).

Nienow, A. W., "Suspension of Solid Particles in Turbine Agitated Baffled Vessels," *Chem. Eng. Sci.*, **23**, 1453 (1968).

Oldshue, J. Y., *Fluid Mixing Technology*, McGraw-Hill, New York (1983).

Oldshue, J. Y., "Current Trends in Mixer Scale-Up Techniques," *Mixing of Liquids by Mechanical Agitation*, J. J. Ulbrecht and G. K. Patterson, eds., Gordon and Breach Sci. Publ., New York (1985).

Randolph, A. D., and M. A. Larson, *Theory of Particulate Processes*, 2nd ed., Academic Press, New York (1988).

Randolph, A. D., and S. K. Sikdar, "Creation and Survival of Secondary Nuclei. The Potassium Sulphate-Water System," *Ind. Eng. Chem. Fundam.*, **15**, 64 (1976).

Tavare, N. S., "Mixing in Continuous Crystallizers," *AIChE J.*, **32**, 705 (1986).

Tavare, N. S., and M. R. Chivate, "Analysis of Batch Evaporative Systems," *Chem. Eng. J.*, **14**, 175 (1977).

Wiker, S. L., and B. E. Anshus, "The Characteristics of a Non-Isothermal Loop Crystallizer," *Chem. Eng. Sci.*, **29**, 1575 (1974).

Zwietering, T. N., "Suspending of Solid Particles in Liquid by Agitators," *Chem. Eng. Sci.*, **8**, 244 (1958).

Manuscript received Apr. 11, 1994, and revision received May 9, 1995.